eLife

Reviewed Preprint
v2 • October 8, 2024
Revised by authors

Reviewed Preprint
v1 • November 28, 2023

Genetics and Genomics

Systematic creation and phenotyping of Mendelian disease models in *C. elegans*: towards large-scale drug repurposing

Thomas J O'Brien, Ida L Barlow, Luigi Feriani, André EX Brown

Institute of Clinical Sciences, Imperial College London, London, UK • MRC London Institute of Medical Sciences, London, UK

Abstract

There are thousands of Mendelian diseases with more being discovered weekly and the majority have no approved treatments. To address this need, we require scalable approaches that are relatively inexpensive compared to traditional drug development. In the absence of a validated drug target, phenotypic screening in model organisms provides a route for identifying candidate treatments. Success requires a screenable phenotype. However, the right phenotype and assay may not be obvious for pleiotropic neuromuscular disorders. Here we show that high- throughput imaging and quantitative phenotyping can be conducted systematically on a panel of *C. elegans* disease model strains. We used CRISPR genome-editing to create 25 worm models of human Mendelian diseases and phenotyped them using a single standardised assay. All but two strains were significantly different from wild-type controls in at least one feature. The observed phenotypes were diverse, but mutations of genes predicted to have related functions led to similar behavioural differences in worms. As a proof-of-concept, we performed a drug repurposing screen of an FDA approved compound library, and identified two compounds that rescued the behavioural phenotype of a model of UNC80 deficiency. Our results show that a single assay to measure multiple phenotypes can be applied systematically to diverse Mendelian disease models. The relatively short time and low cost associated with creating and phenotyping multiple strains suggests that high-throughput worm tracking could provide a scalable approach to drug repurposing commensurate with the number of Mendelian diseases.

eLife Assessment

This **important** study provides proof of principle that C. elegans models can be used to accelerate the discovery of candidate treatments for human Mendelian diseases by detailed high-throughput phenotyping of strains harboring mutations in orthologs of human disease genes. The data are **compelling** and support an approach that enables the potential rapid repurposing of FDA-approved drugs to treat rare diseases for which there are currently no effective treatments. The authors should provide a clearer explanation of how the statistical analyses were performed, as well as a link to a GitHub repository to clarify how figures and tables in the manuscript were generated from the phenotypic data.

https://doi.org/10.7554/eLife.92491.2.sa4

Introduction

By definition, rare genetic diseases each affect a small number of patients

However, because there are many kinds of rare diseases, they are collectively common and affect more than 300 million people worldwide (Nguengang Wakap et al., 2020). Over 80% of rare genetic diseases affect children and many have severe symptoms (Bavisetty et al., 2013). Furthermore, 95% of rare diseases have no approved treatment (Nguengang Wakap et al., 2020). Given the severity and prevalence of rare diseases, the lack of treatments represents an important unmet need. Genome and exome sequencing has become faster and cheaper, enabling its widespread use in the diagnosis of genetic disease. In turn, this has led to the rapid identification of genetic lesions associated with rare genetic diseases (Gonzaga- Jauregui et al., 2012). Genetic diagnosis is an important first step, but often presents patients and physicians with a research problem rather than a treatment.

Genetic diagnoses rarely lead directly to a drug target hypothesis, especially for loss-of-function mutations. In the absence of a validated drug target, phenotypic screens in a model organism provide an alternative route to candidate treatments. Three things are required for a phenotypic screen to be successful: (1) a conserved gene; (2) a genetically tractable organism or culture system in which the disease mutation can be introduced; and (3) a measurable phenotype compatible with high-throughput screening. For the model nematode *C. elegans*, more than half of the human genes associated with rare genetic diseases in the OMIM database are conserved (Kropp et al., 2021) and CRISPR-based editing has made the generation of *in vivo* models containing disease-relevant mutations faster and easier. However, the third condition, a screenable phenotype, remains a bottleneck for many mutations and models.

If all three conditions are met, a phenotypic screen for candidate treatments can be performed. Because there is limited investment in drug development for rare diseases, lead optimisation and safety testing may not be possible. Hence, there is a particular focus on screening approved drugs that have already been shown to be safe and bioavailable in humans to reduce the cost and time it takes to translate screening hits to human trials (Roessler et al., 2021). Two recent examples of promising repurposing screens using multiple model organisms illustrate this potential.

Firstly, modelling amyotrophic lateral sclerosis (ALS) with disease-associated genetic variants of conserved genes in *C. elegans*, zebrafish, and mice led to clinical trials for repurposing of the antipsychotic drug pimozide. By exploiting high throughput drug screening in *C. elegans* carrying

point mutations in *TDP-43*, a panel of drugs were identified that rescued ALS movement and neurodevelopment phenotypes in all animal models. Early clinical trials found pimozide improved clinical and physiological outcomes in ALS patients (Patten et al., 2017). Secondly, the glycosylation disorder, PMM2-CDG, is caused by mutations in *PMM2* and presents clinically with developmental delay, psychomotor retardation, and axial hypotonia, among other symptoms. *C. elegans* carrying the same disease-associated mutation in their endogenous *pmm-2* gene exhibited larval arrest upon pharmacological ER stress. *In vivo* screening identified two compounds that rescued development in *C. elegans* and enzymatic activity in PMM2-CDG patient fibroblasts (Iyer et al., 2019).

One of the compounds, the aldose reductase inhibitor epalrestat, is currently being tested in clinical trials for PMM2-CDG patients (National Clinical Trial number: NCT04925960).

A screenable phenotype was critical for the success of these studies. In the ALS model, worms became paralysed after 2 hours in liquid and in the PMM2-CDG model, brood size was severely affected. The majority (~74%) of rare genetic diseases affect nervous system function (Lee et al., 2020), and many of these mutations will not cause strong effects on development or gross motility when mutated in worms. High-content phenotyping that measures multiple features simultaneously could be useful in these cases to identify differences between strains that are not captured with univariate measures. In this study, we use a combination of high-throughput imaging (Barlow et al., 2022) and quantitative phenotyping (Javer, Currie, et al., 2018; Javer, Ripoll-Sánchez, et al., 2018) to phenotype a diverse panel of 25 *C. elegans* strains with mutations in orthologs of human disease genes. All but two of the mutant strains had detectable phenotypes compared to controls in at least one aspect of their morphology, posture, or motion. No single feature was different in all strains highlighting the need for a multidimensional phenotype. Mutation of genes predicted to have similar functions (e.g., *bbs-1*, *bbs-2,* and *tub-1*) led to similar phenotypes. As a proof-of-concept, we then performed a repurposing screen using a library of 743 FDA approved compounds to identify drugs that improved the behavioural phenotype of *unc-80* loss-of-function mutants. Liranaftate and atorvastatin rescued the core behavioural features associated with *unc-80* loss of function and did not cause a large number of detectable side effects.

The ability to detect phenotypic difference in diverse strains using a standardised 16-minute assay will make it possible to perform repurposing screens for existing and newly described rare diseases efficiently.

Results

Selection and molecular characterisation of a diverse panel of C. elegans disease models

The problem of large-scale disease modelling can be thought of as a problem of sampling and connecting two related genotype-phenotype (GP) maps (**Fig. 1A**). The first is the human disease map. The genomic space is sampled by mutation and mating in humans and the map is elucidated by sequencing and clinical phenotyping of patients with genetic diseases. The second is the model organism map. Here, the genomic space is sampled using mutagenesis and genome editing and the map is elucidated using laboratory experiments. Given the accelerated characterisation of the human GP map, we sought to accelerate the characterisation of the corresponding *C. elegans* GP map. We follow a phenolog-inspired approach to connecting the two maps. Provided there is a causal connection between a genetic variant and a disease in humans and that the causal gene is conserved in worms, the observed worm phenotype may be a useful disease model even if the connection to the human phenotype is non-obvious (McGary et al., 2010).

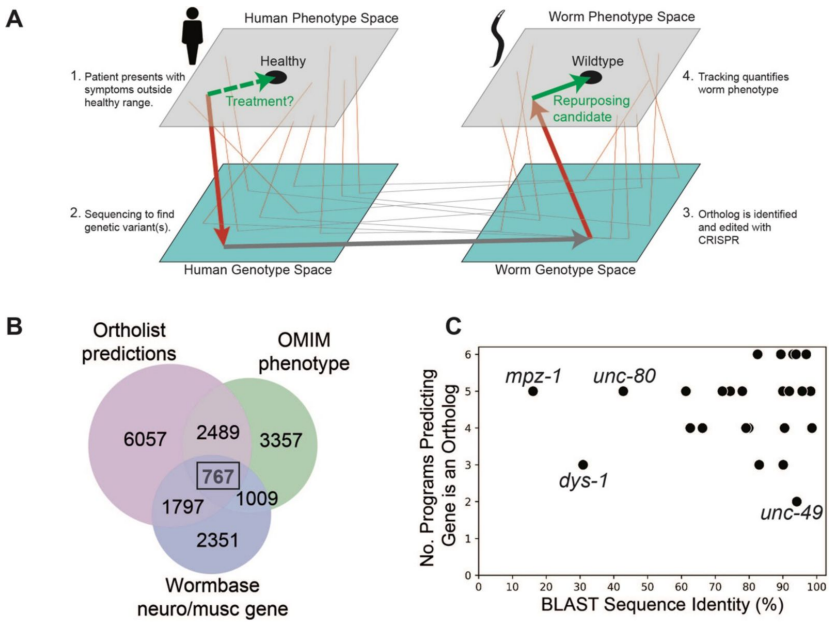

Figure 1

Overview of genotype-phenotype mapping and disease model panel.

Disease modelling as genotype-phenotype mapping in humans and a model organism. Arrows show progression from symptom identification (a phenotype outside the healthy range) to genotyping (placing a patient in genotype space by identifying a genetic variant), disease model creation (making a corresponding mutation in a model organism), and model organism phenotyping. Phenotypic drug screens identify compounds that move a disease model towards the wild-type phenotype (green arrow). These candidates can then be tested in humans (dashed green arrow). Thin lines show other symptom-gene-ortholog-phenotype connections. **(B)** Venn diagram showing number of conserved genes (Ortholist 2), those involved in neuron or muscle function (Wormbase), and those associated with human genetic disorders according to the Online Mendelian Inheritance in Man (OMIM) database. **(C)** Sequence similarity between human and C. elegans genes and the total number of orthology programs predicting that the gene is an ortholog.

To identify a set of *C. elegans* genes that samples a broad genotypic space with connections to the human disease GP map, we first filtered the full database of human-*C. elegans* gene orthologs, Ortholist 2 (Kim et al., 2018), using three criteria: (1) at least two orthology prediction algorithms agree the human and worm genes are orthologs; (2) the WormBase (version WS270) (Harris et al., 2020) gene description includes either 'neuro' or 'musc'; and (3) mutations in the human gene are associated with a Mendelian disease. A total of 767 *C. elegans* genes with 2558 orthologous human protein-coding genes met these criteria (**Figure 1B**). We used keyword searches to further reduce the list to 543 genes. Genes were kept if their WormBase gene description included any of the following: ion, ion channel, dopamine, serotonin, 5-HT, glutamate, acetylcholine, behavior, behaviour, disease, epilepsy, autism, Parkinson, schizophrenia, bipolar, ADHD, seizure, GPCR, coupled receptor, antidepressant, antipsychotic). We prioritised genes associated with autosomal recessive disease in humans to increase the chance that a gene deletion would yield an appropriate model, and we focussed on those where loss-of-function mutants were known or likely to be viable. To get the list of 25 genes presented in this study, the final selection criterion was subjective interestingness based on our prior knowledge, WormBase gene descriptions, and/or brief literature searches.

In the final panel of 25 worm genes selected, 22 genes have >60% sequence similarity to their human ortholog and 11 of the genes share >90% sequence similarity to their human counterpart (**Figure 1C**). Furthermore, 24/25 genes are predicted to be orthologous to human genes across >3 orthology prediction algorithms (**Figure 1C**), and all selected genes have a BLAST E-value (McGinnis & Madden, 2004) smaller than $3x10^{-12}$ (Supplementary Table 1).

Large CRISPR-Cas9 deletions (mean 4.4 kb) were made in each of the target genes to generate 25 strains containing a >55% deletion (average 76%) of the chosen gene. We direct the reader to the strain-specific gene cards (Supplementary Information) for specific details on the size and position of genomic deletions for each of the individual mutants as well as a brief summary of the associated disease and worm phenotypes. Although we have focused on genes expected to have direct effects on neurons or muscles, even this small subset of disease-associated genes is predicted to affect diverse cellular processes including neurotransmission, excitability, development, and cellular structure (**Table 1**). According to OMIM, the mutated genes are associated with 31 rare genetic disorders in humans including intellectual disability, developmental delay, and disorders affecting the muscular and/or nervous systems, and are associated with >70 clinical presentations of disease according to the Human Disease Ontology database (Schriml et al., 2022) (**Table 1**).

Disease-associated mutations result in diverse phenotypes that are captured by multidimensional behavioural fingerprints

Given that there are thousands of rare diseases, methods to characterise the corresponding disease models should be as scalable as possible. Scalability is improved if a single standardised assay can be used to detect model phenotypes regardless of the mutation. High-resolution worm tracking and behavioural fingerprinting is a promising candidate for a widely applicable assay because it is both fast and multidimensional: a single minutes-long recording can capture differences in morphology, posture, and behaviour that can classify the effect of mutations and drug treatments (Baek et al., 2002; Barlow et al., 2022; Geng et al., 2004; Javer, Ripoll-Sánchez, et al., 2018; McDermott-Rouse et al., 2021; Perni et al., 2018; Ramot et al., 2008; Restif et al., 2014; Swierczek et al., 2011; Tsibidis & Tavernarakis, 2007; S. J. Wang & Wang, 2013; Yemini et al., 2013).

We tracked disease model worms on 96-well plates (**Figure 2A**) in three periods: (1) a 5-minute baseline recording (prestim); (2) a 6-minute video with three ten-second blue light stimuli separated by 90 seconds (blue light), and (3) a 5-minute post-stimulus recording (poststim). For

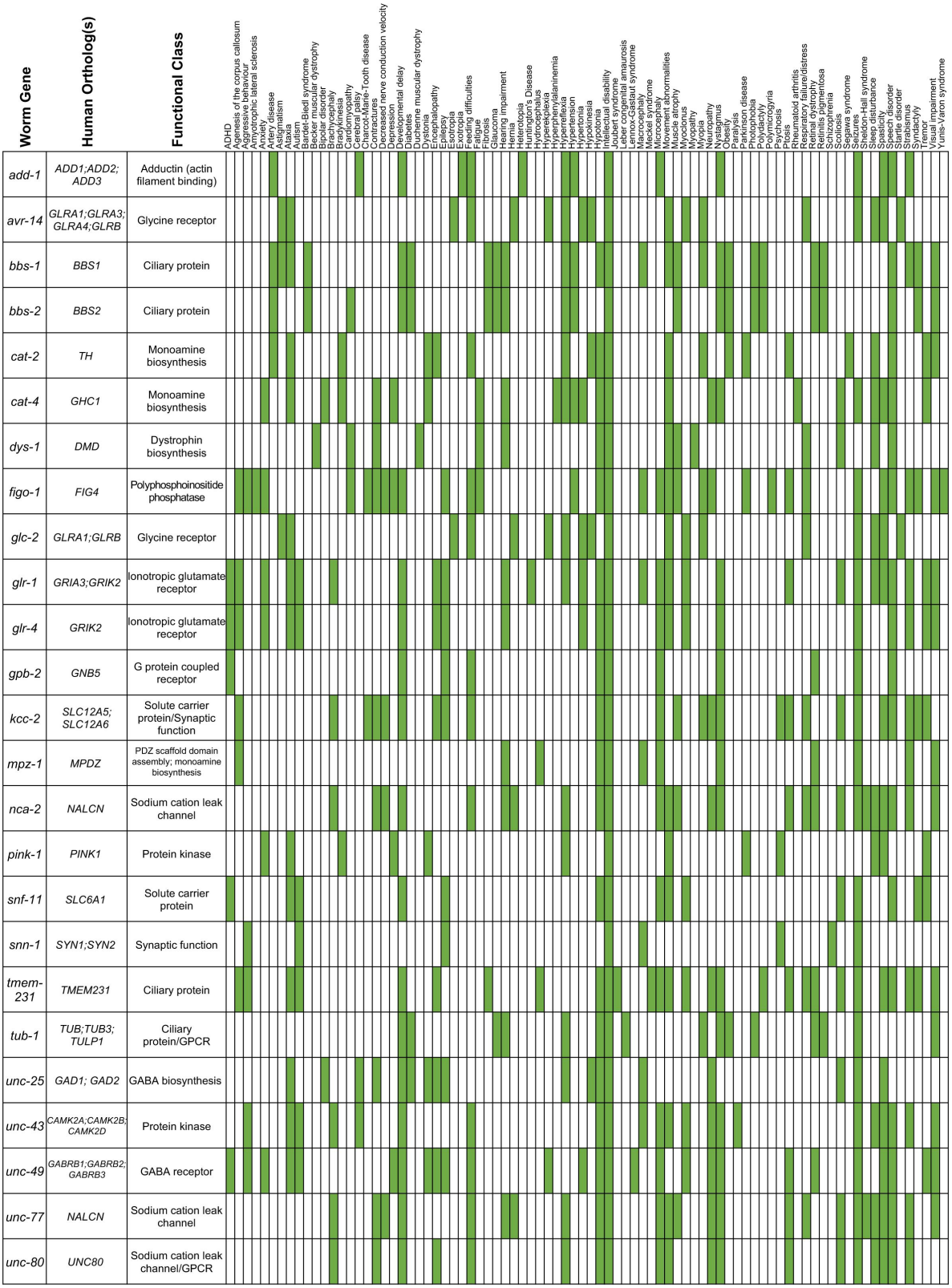

Table 1.

Summary of the associated human ortholog(s), predicted functional class and key associated human disease phenotypes (Human Phenotype Ontology database) for each C. elegans disease model mutant.

each recording we extract 2763 features covering morphology, posture, and motion and concatenate the feature vectors together to represent the phenotype of each strain (8289 features in total). Many of these features are highly correlated and so for clustering we use a pre-selected subset of 256 features (Javer, Ripoll-Sánchez, et al., 2018) (768 across the three recordings). Using these reduced feature vectors, we performed hierarchical clustering across all strains which demonstrates phenotypic diversity (many of the strains are both different from the N2 wild-type strain and from each other) as well as some similarities. For example, *bbs-1*, *bbs-2* and *tub-1* mutants affect cilia formation and result in similar phenotypes that cluster together. The same is true for *kcc-2*, *snf- 11* and *unc-25* mutants, which all affect GABAergic function. An interactive heatmap containing all behavioural feature vectors extracted for every disease model strain is also available for download (*https://doi.org/10.5281/zenodo.12684130*).

Principal component analysis (PCA) of the same data, but now separated into prestimulus, blue light, and poststimlus recordings again shows the separation of many of the mutant strains from the wild-type N2 (**Figure 2D**). The effect of the blue light stimulus on behaviour is clear from the motion of the points through this phenotype space and also reveals new phenotypes. While most strains show a partial recovery in the post-stimulus recording, some strains including *bbs-1*, *bbs-2*, *glr-1*, and *unc-43* display a sustained photophobic response (**Figure 2D**).

From the panel of 25 disease model strains, 23 are significantly different from wild- type in at least one feature (**Figure 2E**). The strains that are most different from wild- type show significant differences across a large number of features. These strains are particularly useful for high-throughput drug screens because the phenotypes can be reliably detected with a small number of replicates. Strain-specific summaries (gene cards) of each disease model mutant, its associated phenotype, and individual molecular characteristics are available in the supplementary information. Here we provide more detailed characterisation of two classes of mutants modelling ciliopathies and channelopathies in humans.

Ciliopathies

Heritable mutations that affect cilia function are associated with a group of rare genetic disorders (ciliopathies) that share diverse symptoms including retinal dystrophy, developmental polydactyly, obesity, cognitive impairment, and renal dysfunction (Reiter & Leroux, 2017). The pleotropic nature of ciliopathies is highlighted by significant interfamilial and intrafamilial phenotypic variability (Shaheen et al., 2016), and the resulting poor gene-phenotype correlation significantly complicates the discovery of effective therapeutics. As a result, current treatment regimens are based on treating individual symptoms.

In the longlist of 543 disease genes, there were 35 genes (6.4% of the total list) predicted to be involved in cilia function. We selected four genes (*bbs-1*, *bbs*-2, *tmem-231* and *tub-1*) involved in regulating nonmotile (primary) cilia development and function that have confirmed expression in the cilia of amphid sensory neurons (Taylor et al., 2021; Ward et al., 2008; Zhang et al., 2022).

Of the genes affecting cilia function, two are orthologs of the Bardet-Biedl syndrome (BBS) family of genes (*bbs-1* and *bbs-2*). BBS is a pleiotropic syndrome often diagnosed in late childhood and is characterised by retinitis pigmentosa, cognitive impairment, obesity, renal dysfunction, hypogonadism, and polydactyly (Forsythe & Beales, 2013). The most prevalent BBS mutations are in *BBS1*, accounting for 23.4% of cases (Forsyth & Gunay-Aygun, 2023), and with 50% embryonic lethality and highly variable phenotypes, *Bbs1-/-* mouse models demonstrate model validity but have not yet yielded insights into potential therapies (Forsyth & Gunay-Aygun, 2023). Mutations in *BBS2* account for 8% of BBS cases (Forsythe & Beales, 2013) and are also implicated in other ciliopathies, such as Meckel syndrome (Karmous-Benailly et al., 2005).

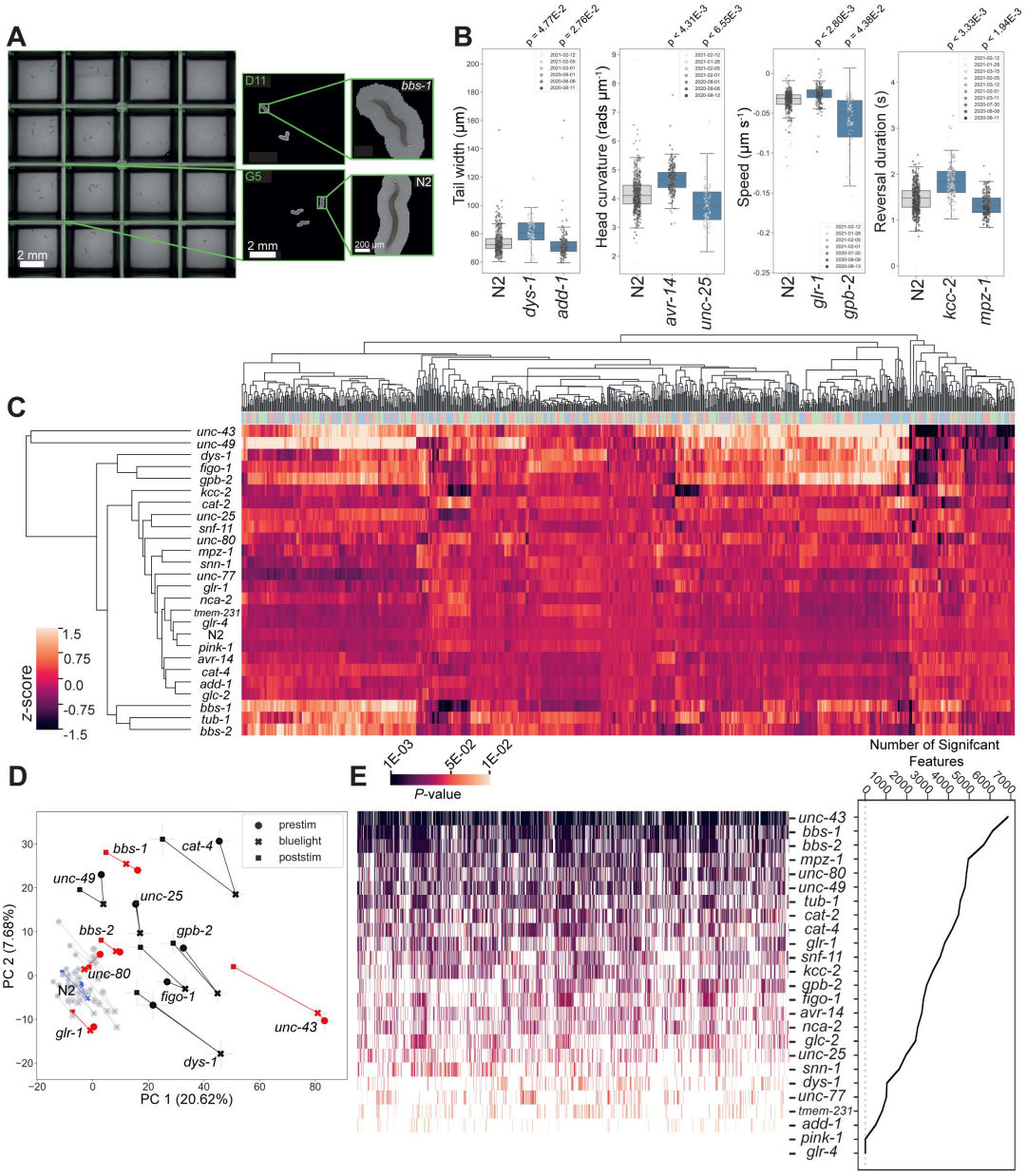

Figure 2

Diverse multidimensional behavioural phenotypes are obtained across the diverse panel of disease model mutants. (A)

Representative field of view for a single camera channel with individual skeletonised worm images of *bbs-1(syb1588)* (top) and N2 (bottom) imaged on the same plate viewed using Tierpsy Tracker. **(B)** Representative behavioural phenotypes extracted by Tierpsy, representing changes in morphology, posture and locomotion of different disease mutant strains. *P*-values are for comparisons to wild-type N2 worms, block permutation t-test, corrected for multiple comparisons. **(C)** Hierarchical clustering of behavioural fingerprints. Features are *Z*-normalised. The top barcode shows the period of image acquisition where the behavioural feature was extracted by Tierpsy: pre-stimulation (pink), blue light (blue) and post-stimulation (green). **(D)** Principal component analysis of the disease model mutants and N2 reference (blue). Strains move in phenospace between pre-stimulus (circular points), blue light (crosses) and post-stimulation (squares) recordings. Strains with an aberrant blue light response are shown in red. Error bars represent standard error of the mean. **(E)** The total number of statistically significant behavioural features for each strain compared to N2 (from the total set of 8289 features extracted by Tierpsy). *P*-values for each feature were calculated using block permutation t-tests, using n = 100,000 permutations and $P < 0.05$ considered statistically significant after correcting for multiple comparisons using the Benjamini-Yekutieli method.

Mutations in *bbs-1* and *bbs-2* led to strong phenotypes including changes in morphology, posture, and locomotion (**Figure 3A-D**). *bbs-1(syb1588)* and *bbs- 2(syb1547)* mutants were shorter, wider, and had decreased curvature compared to wild-type worms (**Figures 3A**, 3B and 3C). They are also hyperactive, with a greater fraction of worms moving during pre-stimulus (baseline) recordings (see individual gene cards), and had faster body bends (derivative of curvature) compared to N2 (**Figure 3D** and **3F**). BBS proteins also regulate the *C. elegans* photoreceptor protein LITE1 in ASH sensory neurons through a DLK-MAPK signalling pathway independent of their function in cilia (Zhang et al., 2022). Consistent with this, we find that *bbs-1(syb1588)* and *bbs-2(syb1547)* mutants have attenuated blue light sensitivity, with both strains exhibiting a delayed forward, but enhance backward photophobic escape response upon 10-second stimulation with blue light (**Figures 3F-H**).

The vertebrate family of tubby-like proteins (TUB, TULP) are required for correct GPCR localisation and intra-flagellar transport in primary cilia (Mukhopadhyay & Jackson, 2011). In humans, mutations in this family are associated with rod-cone dystrophy, obesity, and retinitis pigmentosa (North et al., 1997). Furthermore, *Tub1-/-* mice reflect the associated human disease pleiotropy, with insulin resistance, obesity, and cochlea and visual degeneration (Sun et al., 2012). *C. elegans* have a single ortholog of tubby-like proteins, *tub-1*, and mutants have defects in chemotaxis and insulin signalling as well as increased lipid accumulation (Mak et al., 2006).

tub-1(syb1562) mutants are shorter, wider, and hyperactive compared to wild- type worms, similar to *bbs-1* and *bbs-2* mutants (**Figures 3A**, 3B and 3E). They also have a defect in their response to blue light (**Figures 3F-H**). Unlike BBS mutants, cilia integrity is maintained in *tub-1* loss-of-function mutants (Mak et al., 2006), which could explain the similar but less severe phenotype of *tub-1* mutants compared to *bbs-1* and *bbs-2* mutants.

Compartmentalisation of cilia-specific signalling components is regulated by a complex of transmembrane proteins including TMEM231 and mutations in this compartmentalisation complex are associated with neurodevelopmental limb defects and pathologies of the brain and kidneys found in Joubert and Meckel syndrome (Chih et al., 2012). Mouse *Tmem231-/-* mutations are embryonic lethal and the *C. elegans* ortholog *tmem-231* has been shown to have conserved molecular and cellular function (Roberson et al., 2015). However, unlike the other cilia-related mutants, *tmem-231* mutants do not have significant differences in body morphology or posture compared to N2 (**Figure 3**). We do note that *tmem-231(syb1575)* is slightly more active during baseline tracking (see strain-specific gene card).

Channelopathies

The Na+ cation leak channel (NALCN) is expressed throughout the central nervous system, and in parts of the endocrine (pancreas, adrenal, thyroid gland), respiratory and cardiac systems (Cochet-Bissuel et al., 2014). NALCN is a voltage- independent, nonselective cation channel that regulates resting potential (Senatore et al., 2013), and plays a role in neuromodulation by neurotransmitters (Cochet- Bissuel et al., 2014). Mutations in NALCN are associated with neuromuscular disorders including severe hypotonia, infantile neuroaxonal dystrophy (INAD), congenital contractures, cognitive delay, autism, epilepsy, bipolar disorder, and cardiac/respiratory problems (Aoyagi et al., 2015; Cochet-Bissuel et al., 2014; Gal et al., 2016). NALCN-knock-out mice die 12 hours after birth (Lu et al., 2007), so development of appropriate non-mammalian animal models to understand the associated human diseases is essential.

C. elegans encodes two functionally redundant, but differentially expressed, NALCN homologs, NCA-2 and UNC-77, whose proper expression and axonal localization in cholinergic neurons is regulated by UNC-80 (Zhou et al., 2019). Unlike murine models, *nca-2*, *unc-77*, and *unc-80* loss-of-function mutants are viable. Similar to *Drosophila melanogaster* or mouse neonates lacking the

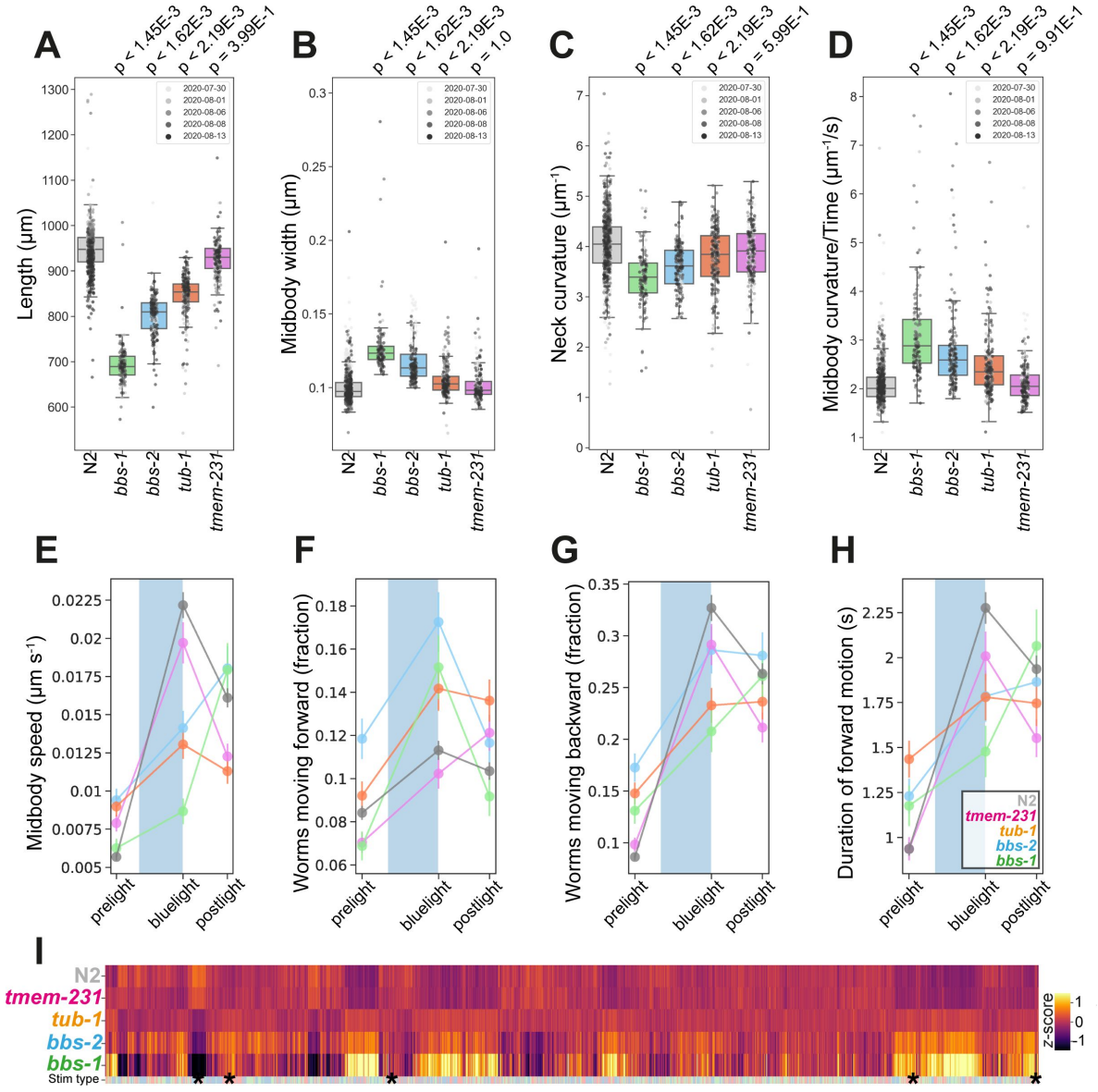

Figure 3

Ciliopathies disease model phenologs. (A-D)

Key behavioural features altered in loss-of-function mutant strains associated with ciliopathies: *bbs-1(syb1588)*, *bbs-2(syb1547)*, *tub-1(syb1562)* and *tmem-231(syb1575)*, under baseline (pre-stimulus) imaging conditions. Individual points marked on the box plots are well averaged values (three worms per well) for each feature across the independent days of tracking. *P*-values are for comparisons to wild-type N2 worms using block permutation t-tests (*n* = 100,000 permutations, correcting for multiple comparisons using the Benjamini-Yekutieli method). **(E-H)** Changes in selected features in response to stimulation with a single 10-second blue light pulse (blue shaded region). Feature values were calculated using 10 second windows centred around 5 seconds before, 10 seconds after, and 20 seconds after the beginning of each blue light pulse. **(I)** Heatmap of the entire set of 8289 behavioural features extracted by Tierpsy for the disease model strains associated with ciliopathies and N2. The 'stim type' barcode denotes when during image acquisition the feature was extracted: pre-stimulation (pink), blue light stimulation (blue) and post-stimulation (green). Asterisks show the location of selected features present in A-E.

cation leak channel (Cochet-Bissuel et al., 2014), loss-of-function mutations in *nca-2* and *unc-80* result in morphological changes in *C. elegans*: both mutants are significantly shorter than wild-type N2 (**Figure 4A**).

Consistent with their differential expression (Jospin et al., 2007; Yeh et al., 2008), we observe phenotypic differences between *nca-2(syb1612)* and *unc- 77(syb1688)* deletion mutants (**Figure 4**). Gain-of-function mutations in *unc-77* have previously been reported to cause deeper body bends (Topalidou et al., 2017) whereas *unc-77(syb1688)* deletion mutants have decreased curvature (**Figure 4B**). In contrast, *nca-2(syb1612)* has no significant change in curvature, but is slower than the wild-type strain (**Figures 4B-C**). We find that *unc-80(syb1531)* mutants, which affect the localisation of NALCN channel subunits, have the most severe phenotype exhibiting a decrease in both curvature and speed (**Figures 4B-4C**).

Mutations in both NALCN channel subunits in *C. elegans* cause a 'fainter' phenotype when stimulated mechanically or immersed in liquid (Pierce-Shimomura et al., 2008). Similarly, we found that a ten second blue light pulse resulted in increased post-exposure pausing and a decreased forward escape response in *nca- 2(syb1612)* and *unc-80(syb1531)* single mutants (**Figures 4E-H**). *unc-77(syb1688)* mutants did not 'faint' after blue light exposure, but consistent with findings that the NALCN channelsome regulates reversal behaviour (Zhou et al., 2019) both *unc- 77(syb1688)* and *unc-80(syb1531)* fail to initiate a backwards escape response.

Pausing and 'fainting' after blue light exposure represents a novel screenable phenotype for NALCN-channelopathies.

Drug repurposing screen in unc-80 mutants

Because *unc-80* mutants have a clear behavioural phenotype without a strong developmental phenotype, we reasoned that they were a useful test case for a drug repurposing screen using an acute 4-hour treatment which might rescue behavioural 'symptoms' in fully developed animals. When screening compound libraries, it is not practical to perform a large number of replicates which would be necessary to detect subtle phonotypes and overcome the reduced statistical power that comes from correcting for multiple comparisons in a large feature set (Supplementary Figure 1). We therefore defined a reduced set of core features to capture the *unc-80* behavioural phenotype consisting of curvature, speed, and fraction of paused worms all during blue light stimulation (**Figure 4B-D**).

For the repurposing screen, we used a library of 743 FDA approved drugs.

We prepared tracking plates where each well contained a drug at a final concentration of 100 μM with 1% DMSO. Three adult worms were added to each well, incubated for 4 hours, and then tracked. The screen was repeated across three independent tracking days with three independent wells per day (9 total well replicates). Hits were defined as compounds that significantly improved all three of the core *unc-80* features, meaning that treated worms were significantly different from *unc-80* DMSO controls and that the direction of the effect was towards wild-type controls. These hit compounds shift *unc-80* towards N2 in a three-dimensional phenotype space (**Figure 5A**). To test the utility of reducing the feature set in a screen compared to testing a larger feature set, we repeated this with larger feature sets. Testing larger feature sets reduced our power to detect differences. No hits were detected using a predefined set of 256 features (Javer, Ripoll-Sánchez, et al., 2018) (Supplementary Figure 1).

We then performed a confirmation screen on 30 of the hit compounds from the initial screen with a larger number of replicates (24 wells per day over three independent days). 13 of the 30 hits were reproduced in the sense of showing significant differences from *unc-80* DMSO controls in the direction of wild-type, however several showed a reduced effect size and were clustered around the *unc- 80* DMSO controls (**Figure 5B**). Having a larger number of replicates, we also tested for

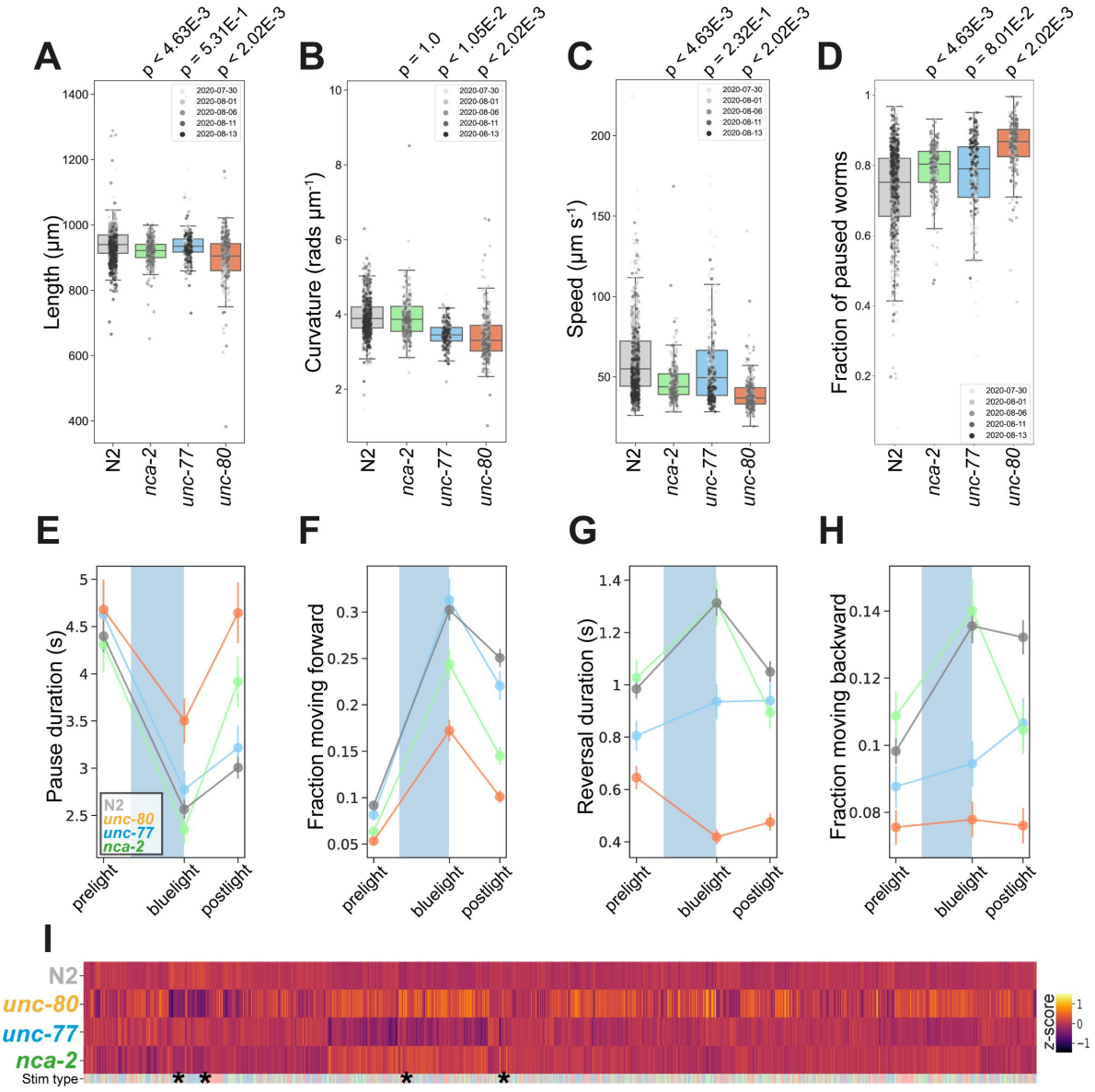

Figure 4

NALCN disease model phenologs. (A-D)

Key behavioural and postural features altered in loss-of-function mutant strains associated with NALCN mutants: *nca-2(syb1612)*, *unc-77(syb1688)* and *unc-80(syb1531)*, under baseline (pre-stimulus) imaging conditions. Individual points marked on the box plots are well averaged values (three worms per well) for each feature across the independent days of tracking. *P*-values are for comparisons to wild-type N2 worms using block permutation t-tests (n = 100,000 permutations correcting for multiple comparisons using the Benjamini-Yekutieli method). **(E-H)** Changes in selected features in response to stimulation with a single 10-second blue light pulse (blue shaded region). Feature values were calculated using 10 second windows centred around 5 seconds before, 10 seconds after, and 20 seconds after the beginning of each blue light pulse. **(E)** A representative 'fainting phenotype' for *unc-80(syb1531)* and *nca-2(syb1612)*, characterised by an increase in pausing following the cessation of stimulation with blue light. **(I)** Heatmap of the entire set of 8289 behavioural features extracted by Tierpsy for the disease model strains associated with NALCN disease and N2. The 'stim type' barcode denotes when during image acquisition the feature was extracted: pre-stimulation (pink), blue light stimulation (blue) and post-stimulation (green). Asterisks show the location of selected features present in A-D.

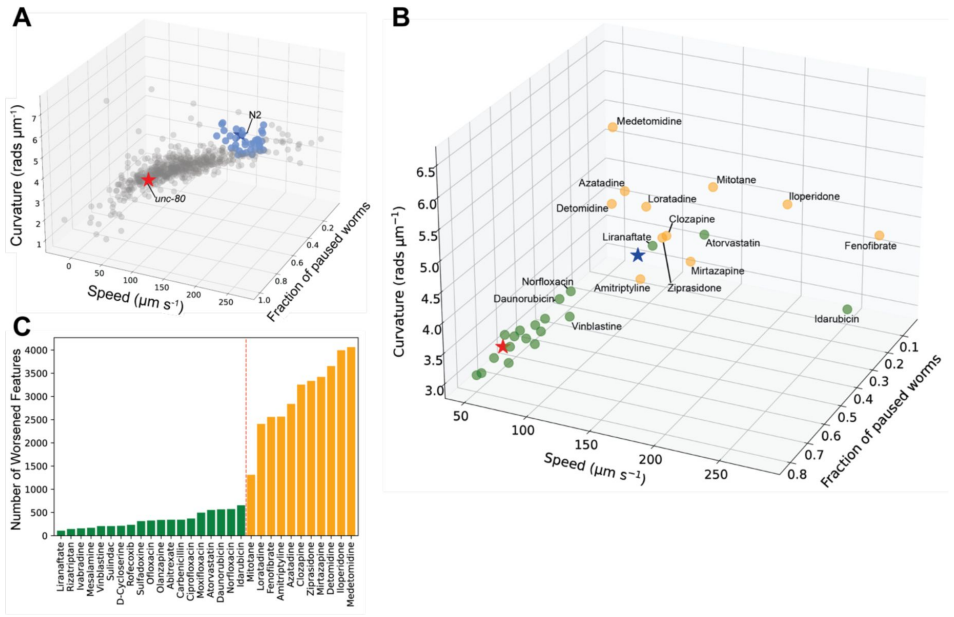

Figure 5

Drug repurposing screening (A)

Phenotypes of unc-80(syb1531) mutant (red star) and N2 (blue star) worms treated with 1% DMSO, and unc-80(syb1531) mutants treated with a library of 743 FDA approved drugs at a concentration of 100 µM for 4 hours (circles). Each point represents an average of 3 well replicates, across 3 independent days of tracking (n = 9 total). Blue points are the top 30 compounds that significantly improved all three of the core behavioural features, pushing the unc-80 mutant strain towards the control in phenospace. **(B)** Confirmation screen of the top 30 compounds identified in the initial library screen. Again unc-80(syb1531) and N2 DMSO treated controls are represented by red and blue stars, respectively, and each circular point represents unc-80(syb1531) treated with 100 µM compound for 4 hours. The 13 compounds coloured in yellow lead to the worsening of >1000 behavioural features (see below). Liranaftate and atorvastatin both lead to a rescue of the core mutant phenotype with a low number of side effects. **(C)** Total number of behavioural side effects following treatment of unc-80(syb1531) with the 30 compounds in the confirmation screen. Side effects are defined as features that are not significant between unc-80 mutants and wild-type N2 worms treated with 1% DMSO but where there is a significant difference between unc-80 mutants treated with a drug compared to N2. Red dashed line separates drug treatments that lead to a worsening of >1000 behavioural features that correspond to the points coloured in yellow in the 3D scatterplot.

'side effects' in treated worms which we define as features where there was no significant difference between *unc-80* mutants and wild-type N2 animals but where there is a significant difference between *unc-80* mutants treated with a drug compared to wild-type N2 animals. About half of the confirmed hit compounds lead to more than 1000 side effects (**Figure 5C**) and are coloured yellow in the core *unc- 80* phenotype space (**Figure 5B**). The same trend is observed when using 256 predefined features (Javer, Ripoll-Sánchez, et al., 2018) (Supplementary Figure 2).

Of the confirmed hit compounds with fewer than 1000 side effects, liranaftate and atorvastatin (Lipitor) lead to good rescue of the core *unc-80* behavioural phenotypes. Interestingly, both compounds act upon the melavonate biosynthesis pathway. The main trunk of this pathway is conserved across species and converts acetyl-CoA to farnesyl diphosphate (Rauthan & Pilon, 2011). Atorvastatin is an inhibitor of HMG-CoA reductase that regulates lipid homeostasis (Goldstein et al., 2006) and catalyses the rate limiting step of the melavonate pathway. Liranaftate, an antifungal inhibitor of squalene epoxidase, shows the greatest behavioural improvement, with the fewest number of side effects. However, *C. elegans* lack the branch of the mevalonate pathway responsible for converting squalene to cholesterol, instead relying on dietary cholesterol. In this case the effect may be due to an off-target interaction on one of the other enzymes in the pathway.

Fenofibrate, a PPAR-alpha activator that increases lipolysis, is also a hit but has a large number of side effects. Given that it overshoots perfect rescue by shifting *unc-80* animals past wild-type controls in core phenospace, it could be that at a lower dose it would provide good rescue with fewer side effects. Since UNC-80 is involved in localisation of the NACLN+ channel complex, we hypothesise that changes in membrane composition might be indirectly affecting the localisation or function of the channel complex.

Discussion

We framed the problem of disease modelling as one of sampling and elucidating a model organism genotype-phenotype map that is connected to a human disease genotype-phenotype map through genetic conservation. However, both the genomic and phenomic spaces are large and high-dimensional and so it was not clear that a systematic approach would identify useful phenologs for disease modelling. Using an initial set of genes that are diverse in function (but biased towards roles in neurons and muscles) and that lead to diverse symptoms when mutated in humans, we found that it is possible to systematically create and phenotype worm models of rare diseases using a uniform assay and protocol. Without adding additional perturbations or experimental conditions, we found that 23 out of the 25 disease models we made had detectable differences compared to the wild-type.

Of the disease models with detectable phenotypes, approximately half had strong phenotypes that would support high throughput phenotypic screens for candidate treatments. To test the feasibility of performing drug repurposing screens using the same uniform assay, we chose a worm model of UNC80 deficiency and, focussing on a reduced core phenotype, identified an initial list of 30 FDA-approved drugs that rescued the mutant phenotype. A confirmation screen with more replicates identified several compounds that still rescued the core disease model phenotype and did not have a large number of side effects. For UNC80 deficiency we chose a short treatment time of four hours to model treatment in patients where some developmental effects will have already occurred. Our approach is also compatible with longer treatments where animals at the first larval stage are added to tracking plates and allowed to develop in the presence of drugs. This might reveal other hit compounds and would be particularly interesting for mutants with developmental delays including some in this study (e.g. *cat-4*, *dys-1*, *figo-1*, *gpb-2* and *kcc-2*).

For this proof-of-principle study, we focused on the generation of large deletion alleles to help ensure the target gene is functionally disrupted. However, patient-specific missense mutations can also be introduced at conserved loci within genes and these mutations can lead to detectable behavioural phenotypes (see for example (Barlow et al., 2022; D. Wang et al., 2021)). There is also value in studying multiple alleles even for loss-of-function mutations. The large deletions we use here can delete regulatory elements or non-coding RNAs that could lead to phenotypes not related to the modelled disease. Alternative methods of creating loss-of-function alleles such as introducing premature stop codons can also be done at the scale of dozens of strains (Pu et al., 2023). Furthermore, to study loss of function in essential genes, balanced heterozygous strains can be created where this makes sense for a particular disease model.

With a current discovery rate of >100 new genetic diseases each year, the number of diseases with little aetiological understanding is going to grow at a faster rate than biomedical and pharmaceutical research will find therapies (Boycott et al., 2017). Therefore, novel approaches that can systematically screen the effects of large numbers of genetic variants associated with different diseases are required. CRISPR genome editing in model organisms including *C. elegans* allows the creation of new disease models at the required rate and cost. We have shown that high-throughput worm tracking can identify screenable phenotypes and be used for repurposing screens. However, we do not yet know whether the phenotypes and repurposing hits will be useful for translation. It is possible that the phenotypes we detect are not direct results of key disease mechanisms but are instead secondary effects on connected systems. We expect that secondary effects are less likely to be driven by conserved mechanisms but this can only be assessed on a case-by-base basis. Similarly, the 'side effects' we detect in worms may not be predictive in humans. Still, we think quantifying side effects will be useful in some cases. For example, if a disease model is hyperactive and gross motility were the only measure used in a screen, compounds that are broadly toxic would be detected as hits. This kind of broad toxicity would result in a large number of side effects and could be avoided. Ultimately, the translatability of hits in invertebrate screens can only be determined in clinical trials and choosing hits from phenotypic screens to pursue clinically will require judgement that takes into account the full picture available from multiple data sources including the strength of rescue, the putative drug mechanism of action, knowledge of disease biology, and an assessment of the risk of testing a given drug in patients. We are optimistic that we will see more human trials based on screens in diverse small animal models.

Materials and Methods

Mutant generation

CRISPR guide RNAs were designed to target large deletions (>1000bp) that start close to the start codon and excise several exons from the gene in order to give high confidence of loss of function. For exceptionally large genes (e.g. *dys-1* or *mpz-1*) the entire protein-coding region was excised. Mutants were designed and made by SunyBiotech in an N2 background.

Worm preparation

All strains were cultured on Nematode Growth Medium at 20°C and fed with *E. coli* (OP50) following standard procedure (Stiernagle, 2006). Synchronised populations of young adult worms for imaging were cultured by bleaching unsynchronised gravid adults, and allowing L1 diapause progeny to develop for 2.5 days at 20°C (detailed protocol: *https://dx.doi.org/10.17504/protocols.io.2bzgap6*). Several strains were developmentally delayed and were allowed to grow for longer before imaging. *cat- 4*(*syb1591*), *gpb-2*(*syb1577*), *kcc-2*(*syb2673*), and *unc-25*(*syb1651*) were allowed to develop for 3.5 and *dys-1*(*syb1688*), *figo-1*(*syb1562*), and *pink-1*(*syb1546*) were allowed to develop for 5.5 days prior to imaging. On the day of imaging, young adults were washed in M9 (detailed protocol: *https://dx.doi.org/10.17504/protocols.io.bfqbjmsn*), transferred to the

imaging plates (3 worms per well) using a COPAS 500 Flow Pilot (detailed protocol: *https://dx.doi.org/10.17504/protocols.io.bfc9jiz6*), and returned to a 20°C incubator for 3.5 hours. Plates were then transferred onto the multi-camera tracker for another 30 minutes to habituate prior to imaging (detailed protocol: *https://dx.doi.org/10.17504/protocols.io.bsicncaw*).

For drug repurposing experiments, the MRCT FDA-approved compound library (Catalog No.L1300) was supplied pre-dissolved in DMSO by LifeArc (Stevenage, UK). The day prior to tracking, imaging plates were dosed with the compound library to achieve a final well concentration of 100 µM prior to seeding with bacteria (see below for details). Plates were left to dry (~30 mins), before being stored in the dark at room temperature overnight. Following the methods described above, age synchronized young adult *unc-80*(*syb1531*) worms were dispensed into the imaging plate wells and incubated at 20°C for 4 hours before tracking. The behaviour of mutant worms dosed with the drugs was then compared to wild-type N2 and *unc-80*(*syb1531*) worms (also age-synchronized young adults) dispensed into the wells of the same tracking plates dosed with an identical volume (1% w/v) of DMSO only (detailed protocol: *https://dx.doi.org/10.17504/protocols.io.5jyl8p5yrg2w/v1*).

Plate preparation

Low peptone (0.013%) nematode growth medium (detailed protocol: *https://dx.doi.org/10.17504/protocols.io.2rcgd2w*) was prepared as follows: 20 g agar (Difco), 0.13 g Bactopeptone, and 3 g NaCl were dissolved in 975 mL of milliQ water. After autoclaving, 1 mL of 10 mg/mL cholesterol was added along with 1 mL CaCl2 (1 M), 1 mL MgSO4 (1 M) and 25 mL KPO4 buffer (1M, pH 6.0). Molten agar was cooled to 50-60°C and 200 µL was dispensed into each well of 96-square well plates (Whatman UNIPLATE: WHAT-77011651) using an Integra VIAFILL (detailed protocol: *https://dx.doi.org/10.17504/protocols.io.bmxbk7in*). Poured plates were stored agar-side up at 4°C until required.

One day prior to imaging, plates were placed without lids in a drying cabinet to lose 3-5% of weight by volume. Wells were then seeded with 5 µL OP50 (OD600 1.0) using an Integra VIAFILL dispenser, and plates were stored with lids (WHAT- 77041001) on at room temperature overnight.

Image acquisition

All videos were acquired and processed following methods previously described (Barlow et al., 2022). In brief, videos were acquired at 25 frames per second in a room with a nominal temperature of 20°C using a shutter time of 25 ms and a resolution of 12.4 µm/px. Three videos were taken sequentially: a 5-minute pre- stimulus video, a 6-minute blue light recording with three 10-second blue light pulses starting at 60, 160 and 260 seconds, and a 5-minute post-stimulus recording. The script for controlling recording timings and photostimulation was made using LoopBio's API for their Motif software (*https://github.com/loopbio/python-motifapi*).

Image processing and feature extraction

Videos were segmented and tracked using Tierpsy Tracker (Javer, Currie, et al., 2018). After segmentation of worm skeletons, our previously described convolutional neural network classifier was used to exclude non-worm objects from being classified during feature extraction (Barlow et al., 2022). Skeletons that did not meet the following criteria were removed from the analysis: 700 – 1300 µM length, 20 – 200 µM width. As an additional quality control measure, we used Tierpsy Tracker's viewer to mark wells with visible contamination, agar damage, compound precipitation, or excess liquid as "bad", and exclude these wells from downstream analysis.

Following tracking, we extracted a previously-defined set of 3076 behavioural features for each well in each of the three videos (pre-stimulus, blue light, and post- stimulus) (Javer, Ripoll-Sánchez, et al., 2018). Feature values are averaged over tracks to produce a single feature vector for each

well.

Statistical analysis

Statistically significant differences in the pre-stimulus, post-stimulus and blue-light behavioural feature sets extracted from each disease model strain compared to our N2 reference were calculated using block permutation t-tests (*https://github.com/Tierpsy/tierpsy-tools-python/blob/master/tierpsytools/analysis/statistical_tests.py*). Python (version 3.8.5) was used to perform the analysis, using n = 10000 permutations that were randomly shuffled within, but not between, the independent days of image acquisition for each strain to control for day-to-day variation in the experiments. The p-values were then corrected for multiple comparisons using the Benjamini-Yekutieli procedure to control the false discovery rate at 5% (Benjamini & Yekutieli, 2001).

Heatmaps, cluster maps and principal component analysis of the extracted feature sets for each disease model strain compared to our N2 reference were calculated using in-built Seaborn (version 0.11.2) packages (Waskom, 2021). All scripts used for statistical analysis and the generation of figures are available at: *https://github.com/Tom-OBrien/Disease-Modelling*.

Data Availability

The datasets (Tierpsy features, tracking data, and metadata) produced in this study are available on Zenodo: *https://doi.org/10.5281/zenodo.12684118*. Any remaining information can be obtained from the corresponding author upon reasonable request.

Acknowledgements

This project has received funding from the European Research Council (ERC) under the European Union's Horizon 2020 research and innovation programme (Grant agreement No. 714853) and was supported by the Medical Research Council through grant MC-A658-5TY30.

References

1. Aoyagi K., Rossignol E., Hamdan F. F., Mulcahy B., Xie L., Nagamatsu S., Rouleau G. A., Zhen M., Michaud J. L (2015) **A Gain-of-Function Mutation in NALCN in a Child with Intellectual Disability, Ataxia, and Arthrogryposis** *Human Mutation* **36**:753–757 https://doi.org/10.1002/humu.22797

2. Baek J.-H., Cosman P., Feng Z., Silver J., Schafer W. R (2002) **Using machine vision to analyze and classify Caenorhabditis elegans behavioral phenotypes quantitatively** *Journal of Neuroscience Methods* **118**:9–21 https://doi.org/10.1016/S0165-0270(02)00117-6

3. Barlow I. L. *et al.* (2022) **Megapixel camera arrays enable high-resolution animal tracking in multiwell plates** *Communications Biology* **5** https://doi.org/10.1038/s42003-022-03206-1

4. Bavisetty S., Grody W. W., Yazdani S (2013) **Emergence of pediatric rare diseases: Review of present policies and opportunities for improvement** *Rare Diseases* **1** https://doi.org/10.4161/rdis.23579

5. Benjamini Y., Yekutieli D (2001) **The control of the false discovery rate in multiple testing under dependency** *The Annals of Statistics* **29**:1165–1188 https://doi.org/10.1214/aos/1013699998

6. Boycott K. M. *et al.* (2017) **International Cooperation to Enable the Diagnosis of All Rare Genetic Diseases** *The American Journal of Human Genetics* **100**:695–705 https://doi.org/10.1016/j.ajhg.2017.04.003

7. Chih B., Liu P., Chinn Y., Chalouni C., Komuves L. G., Hass P. E., Sandoval W., Peterson A. S (2012) **A ciliopathy complex at the transition zone protects the cilia as a privileged membrane domain** *Nature Cell Biology* **14** https://doi.org/10.1038/ncb2410

8. Cochet-Bissuel M., Lory P., Monteil A (2014) **The sodium leak channel, NALCN, in health and disease** *Frontiers in Cellular Neuroscience* **8**

9. Forsyth R., Gunay-Aygun M., Adam M. P., Mirzaa G. M., Pagon R. A., Wallace S. E., Bean L. J., Gripp K. W., Amemiya A. (2023) **Bardet-Biedl Syndrome Overview** *GeneReviews®*

10. Forsythe E., Beales P. L (2013) **Bardet–Biedl syndrome** *European Journal of Human Genetics* **21** https://doi.org/10.1038/ejhg.2012.115

11. Gal M., Magen D., Zahran Y., Ravid S., Eran A., Khayat M., Gafni C., Levanon E. Y., Mandel H (2016) **A novel homozygous splice site mutation in NALCN identified in siblings with cachexia, strabismus, severe intellectual disability, epilepsy and abnormal respiratory rhythm** *European Journal of Medical Genetics* **59**:204–209 https://doi.org/10.1016/j.ejmg.2016.02.007

12. Geng W., Cosman P., Berry C. C., Feng Z., Schafer W. R (2004) **Automatic tracking, feature extraction and classification of C elegans phenotypes** *IEEE Transactions on Bio-Medical Engineering* **51**:1811–1820 https://doi.org/10.1109/TBME.2004.831532

13. Goldstein J. L., DeBose-Boyd R. A., Brown M. S (2006) **Protein sensors for membrane sterols** *Cell* **124**:35–46 https://doi.org/10.1016/j.cell.2005.12.022

14. Gonzaga-Jauregui C., Lupski J. R., Gibbs R. A (2012) **Human genome sequencing in health and disease** *Annual Review of Medicine* **63**:35–61 https://doi.org/10.1146/annurev-med-051010-162644

15. Harris T. W. *et al.* (2020) **WormBase: A modern Model Organism Information Resource** *Nucleic Acids Research* **48**:D762–D767 https://doi.org/10.1093/nar/gkz920

16. Iyer S. *et al.* (2019) **Repurposing the aldose reductase inhibitor and diabetic neuropathy drug epalrestat for the congenital disorder of glycosylation PMM2-CDG** *Disease Models & Mechanisms* **12**:11 https://doi.org/10.1242/dmm.040584

17. Javer A. *et al.* (2018) **An open source platform for analyzing and sharing worm behavior data** *Nature Methods* **15**:645–646 https://doi.org/10.1038/s41592-018-0112-1

18. Javer A., Ripoll-Sánchez L., Brown A. E. X (2018) **Powerful and interpretable behavioural features for quantitative phenotyping of Caenorhabditis elegans** *Philosophical Transactions of the Royal Society B: Biological Sciences* **373** https://doi.org/10.1098/rstb.2017.0375

19. Jospin M., Watanabe S., Joshi D., Young S., Hamming K., Thacker C., Snutch T. P., Jorgensen E. M., Schuske K (2007) **UNC-80 and the NCA ion channels contribute to endocytosis defects in synaptojanin mutants** *Current Biology: CB* **17**:1595–1600 https://doi.org/10.1016/j.cub.2007.08.036

20. Karmous-Benailly H. *et al.* (2005) **Antenatal Presentation of Bardet-Biedl Syndrome May Mimic Meckel Syndrome** *American Journal of Human Genetics* **76**:493–504

21. Kim W., Underwood R. S., Greenwald I., Shaye D. D (2018) **OrthoList 2: A New Comparative Genomic Analysis of Human and Caenorhabditis elegans Genes** *Genetics* **210**:445–461 https://doi.org/10.1534/genetics.118.301307

22. Kropp P. A., Bauer R., Zafra I., Graham C., Golden A (2021) **Caenorhabditis elegans for rare disease modeling and drug discovery: Strategies and strengths** *Disease Models & Mechanisms* **14**:8 https://doi.org/10.1242/dmm.049010

23. Lee C. E., Singleton K. S., Wallin M., Faundez V (2020) **Rare Genetic Diseases: Nature's Experiments on Human Development** *iScience* **23** https://doi.org/10.1016/j.isci.2020.101123

24. Lu B., Su Y., Das S., Liu J., Xia J., Ren D (2007) **The neuronal channel NALCN contributes resting sodium permeability and is required for normal respiratory rhythm** *Cell* **129**:371–383 https://doi.org/10.1016/j.cell.2007.02.041

25. Mak H. Y., Nelson L. S., Basson M., Johnson C. D., Ruvkun G (2006) **Polygenic control of Caenorhabditis elegans fat storage** *Nature Genetics* **38** https://doi.org/10.1038/ng1739

26. McDermott-Rouse A., Minga E., Barlow I., Feriani L., Harlow P. H., Flemming A. J., Brown A. E. X (2021) **Behavioral fingerprints predict insecticide and anthelmintic mode of action** *Molecular Systems Biology* **17** https://doi.org/10.15252/msb.202110267

27. McGary K. L., Park T. J., Woods J. O., Cha H. J., Wallingford J. B., Marcotte E. M (2010) **Systematic discovery of nonobvious human disease models through orthologous phenotypes** *Proceedings of the National Academy of Sciences* **107**:6544–6549 https://doi.org/10.1073/pnas.0910200107

28. McGinnis S., Madden T. L (2004) **BLAST: At the core of a powerful and diverse set of sequence analysis tools** *Nucleic Acids Research* **32**:W20–W25 https://doi.org/10.1093/nar/gkh435

29. Mukhopadhyay S., Jackson P. K (2011) **The tubby family proteins** *Genome Biology* **12** https://doi.org/10.1186/gb-2011-12-6-225

30. Wakap S. N., Lambert D. M., Olry A., Rodwell C., Gueydan C., Lanneau V., Murphy D., Le Cam Y., Rath A. (2020) **Estimating cumulative point prevalence of rare diseases: Analysis of the Orphanet database** *European Journal of Human Genetics* **28** https://doi.org/10.1038/s41431-019-0508-0

31. North M. A., Naggert J. K., Yan Y., Noben-Trauth K., Nishina P. M (1997) **Molecular characterization of TUB, TULP1, and TULP2, members of the novel tubby gene family and their possible relation to ocular diseases** *Proceedings of the National Academy of Sciences of the United States of America* **94**:3128–3133

32. Patten S. A. *et al.* (2017) **Neuroleptics as therapeutic compounds stabilizing neuromuscular transmission in amyotrophic lateral sclerosis** *JCI Insight* **2** https://doi.org/10.1172/jci.insight.97152

33. Perni M. *et al.* (2018) **Massively parallel C. elegans tracking provides multi-dimensional fingerprints for phenotypic discovery** *Journal of Neuroscience Methods* https://doi.org/10.1016/j.jneumeth.2018.02.005

34. Pierce-Shimomura J. T., Chen B. L., Mun J. J., Ho R., Sarkis R., McIntire S. L (2008) **Genetic analysis of crawling and swimming locomotory patterns in C. elegans** *Proceedings of the National Academy of Sciences of the United States of America* **105**:20982–20987 https://doi.org/10.1073/pnas.0810359105

35. Pu L. *et al.* (2023) **Dissecting the genetic landscape of GPCR signaling through phenotypic profiling in C. elegans** *Nature Communications* **14** https://doi.org/10.1038/s41467-023-44177-z

36. Ramot D., Johnson B. E., Berry T. L., Carnell L., Goodman M. B (2008) **The Parallel Worm Tracker: A Platform for Measuring Average Speed and Drug-Induced Paralysis in Nematodes** *PLoS ONE* **3** https://doi.org/10.1371/journal.pone.0002208

37. Rauthan M., Pilon M (2011) **The mevalonate pathway in C. Elegans** *Lipids in Health and Disease* **10** https://doi.org/10.1186/1476-511X-10-243

38. Reiter J. F., Leroux M. R (2017) **Genes and molecular pathways underpinning ciliopathies** *Nature Reviews Molecular Cell Biology* **18** https://doi.org/10.1038/nrm.2017.60

39. Restif C., Ibáñez-Ventoso C., Vora M. M., Guo S., Metaxas D., Driscoll M (2014) **CeleST: Computer vision software for quantitative analysis of C. elegans swim behavior reveals novel features of locomotion** *PLoS Computational Biology* **10** https://doi.org/10.1371/journal.pcbi.1003702

40. Roberson E. C. *et al.* (2015) **TMEM231, mutated in orofaciodigital and Meckel syndromes, organizes the ciliary transition zone** *The Journal of Cell Biology* **209** https://doi.org/10.1083/jcb.201411087

41. Roessler H. I., Knoers N. V. A. M., van Haelst M. M., van Haaften G. (2021) **Drug Repurposing for Rare Diseases** *Trends in Pharmacological Sciences* **42**:255–267 https://doi.org/10.1016/j.tips.2021.01.003

42. Schriml L. M. *et al.* (2022) **The Human Disease Ontology 2022 update** *Nucleic Acids Research* **50**:D1255–D1261 https://doi.org/10.1093/nar/gkab1063

43. Senatore A., Monteil A., van Minnen J., Smit A. B., Spafford J. D. (2013) **NALCN Ion Channels Have Alternative Selectivity Filters Resembling Calcium Channels or Sodium Channels** *PLOS ONE* **8** https://doi.org/10.1371/journal.pone.0055088

44. Shaheen R. *et al.* (2016) **Characterizing the morbid genome of ciliopathies** *Genome Biology* **17** https://doi.org/10.1186/s13059-016-1099-5

45. Stiernagle T (2006) **Maintenance of C. elegans** *WormBook: The Online Review of C. Elegans Biology* https://doi.org/10.1895/wormbook.1.101.1

46. Sun X., Haley J., Bulgakov O. V., Cai X., McGinnis J., Li T (2012) **Tubby is required for trafficking G protein-coupled receptors to neuronal cilia** *Cilia* **1** https://doi.org/10.1186/2046-2530-1-21

47. Swierczek N. A., Giles A. C., Rankin C. H., Kerr R. A (2011) **High-throughput behavioral analysis in C. elegans** *Nature Methods* **8**:592–598 https://doi.org/10.1038/nmeth.1625

48. Taylor S. R. *et al.* (2021) **Molecular topography of an entire nervous system** *Cell* **184**:4329–4347 https://doi.org/10.1016/j.cell.2021.06.023

49. Topalidou I., Cooper K., Pereira L., Ailion M (2017) **Dopamine negatively modulates the NCA ion channels in C. elegans** *PLoS Genetics* **13** https://doi.org/10.1371/journal.pgen.1007032

50. Tsibidis G. D., Tavernarakis N (2007) **Nemo: A computational tool for analyzing nematode locomotion** *BMC Neuroscience* **8** https://doi.org/10.1186/1471-2202-8-86

51. Wang D., Dao M., Muntean B. S., Giles A. C., Martemyanov K. A., Grill B (2021) **Genetic modeling of GNAO1 disorder delineates mechanisms of Gαo dysfunction** *Human Molecular Genetics* **31**:510–522 https://doi.org/10.1093/hmg/ddab235

52. Wang S. J., Wang Z.-W (2013) **Track-A-Worm** *An Open-Source System for Quantitative Assessment of C. elegans Locomotory and Bending Behavior. PLoS ONE* **8** https://doi.org/10.1371/journal.pone.0069653

53. Ward A., Liu J., Feng Z., Xu X. Z. S (2008) **Light-sensitive neurons and channels mediate phototaxis in C. elegans** *Nature Neuroscience* **11** https://doi.org/10.1038/nn.2155

54. Waskom M. L (2021) **seaborn: Statistical data visualization** *Journal of Open Source Software* **6** https://doi.org/10.21105/joss.03021

55. Yeh E. *et al.* (2008) **A putative cation channel, NCA-1, and a novel protein, UNC-80, transmit neuronal activity in C. elegans** *PLoS Biology* **6** https://doi.org/10.1371/journal.pbio.0060055

56. Yemini E., Jucikas T., Grundy L. J., Brown A. E. X., Schafer W. R (2013) **A database of Caenorhabditis elegans behavioral phenotypes** *Nature Methods* **10**:877–879 https://doi.org/10.1038/nmeth.2560

57. Zhang X., Liu J., Pan T., Ward A., Liu J., Xu X. Z. S (2022) **A cilia-independent function of BBSome mediated by DLK-MAPK signaling in C. elegans photosensation** *Developmental Cell* **57**:1545–1557 https://doi.org/10.1016/j.devcel.2022.05.005

58. Zhou C., Luo J., He X., Zhou Q., He Y., Wang X., Ma L (2019) **The NALCN Channel Regulator UNC-80 Functions in a Subset of Interneurons To Regulate Caenorhabditis elegans Reversal Behavior** *G3: Genes|Genomes|Genetics* **10** https://doi.org/10.1534/g3.119.400692

Editors

Reviewing Editor
Patrick Hu
Vanderbilt University Medical Center, Nashville, United States of America

Senior Editor
Tony Yuen
Icahn School of Medicine at Mount Sinai, New York, United States of America

Reviewer #1 (Public review):

Summary:

As the scientific community identifies increasing numbers of genes and genetic variants that cause rare human diseases, a challenge in the field quickly identify pharmacological interventions to address known deficits. The authors point out that defining phenotypic outcomes required for drug screen assays is often a bottleneck, and emphasize how invertebrate models can be used for quick ID of compounds that may address genetic deficits. A major contribution of this work is to establish a framework for potential intervention drug screening based on quantitative imaging of morphology and mobility behavior, using methods that the authors show can define subtle phenotypes in a high proportion of disease gene knockout mutants. Overall, the work constitutes an elegant combination of previously developed high-volume imaging with highly detailed quantitative phenotyping (and some paring down to specific phenotypes) to establish proof of principle on how the combined applications can contribute to screens for compounds that may address specific genetic deficits, which can, in turn, suggest both mechanism and therapy.

In brief, the authors selected 25 genes for which loss of function is implicated in human neuro-muscular disease and engineered deletions in the corresponding C. elegans homologs. The authors then imaged morphological features and behaviors prior to, during, and after blue light stimuli, quantitating features, and clustering outcomes as they elegantly developed previously (PMID 35322206; 30171234; 30201839). In doing so, phenotypes in 23/25 tested mutants could be separated enough to distinguish WT from mutant and half of those with adequate robustness to permit high-throughput screens, an outcome that supports the utility of related general efforts to ID phenotypes in C. elegans disease orthologs. A detailed discussion of 4 ciliopathy gene defects, and NACLN-related channelopathy mutants reveals both expected and novel phenotypes, validating the basic approach to modeling vetted targets and underscoring that quantitative imaging approaches reiterate known biology.

The authors then screened a library of nearly 750 FDA-approved drugs for the capacity to shift the unc-80 NACLN channel-disrupted phenotype closer to the wild type. Top "mover" compounds shift outcome in the experimental outcome space; and also reveal how "side effects" can be evaluated to prioritize compounds that confer the fewest changes of other parameters away from the center.

Strengths:

Although the imaging and data analysis approaches have been reported and the screen is restricted in scope and intervention exposure, it is impressive, encouraging and important that the authors strongly combine tools to demonstrate how quantitative imaging phenotypes can be integrated with C. elegans genetics to accelerate the identification of potential modulators of disease (easily extendable to other goals). Generation of deletion alleles and documentation of their associated phenotypes (available in supplemental data) provide potentially useful reagents/data to the field. The capacity to identify "over-shooting" of compound applications with suggestions for scale back and to sort efficacious interventions to minimize other changes to behavioral and physical profiles is a strong contribution.

Weaknesses:

The work does not have major weaknesses, and in revision, the authors have expanded the discussion to potential utility and application in the field.

The authors have also taken into account minor modifications in writing.

https://doi.org/10.7554/eLife.92491.2.sa3

Reviewer #2 (Public review):

Summary and strengths:

O'Brien et al. present a compelling strategy to both understand rare disease that could have a neuronal focus and discover drugs for repurposing that can affect rare disease phenotypes. Using C. elegans, they optimize the Brown lab worm tracker and Tierpsy analysis platform to look at movement behaviors of 25 knockout strains. These gene knockouts were chosen based on a process to identify human orthologs that could underlie rare diseases. I found the manuscript interesting and a powerful approach to make genotype-phenotype connections using C. elegans. Given the rate that rare Mendelian diseases are found and candidate genes suggested, human geneticists need to consider orthologous approaches to understand the disease and seek treatments on a rapid time scale. This approach is one such way. Overall, I have a few minor suggestions and some specific edits.

Weaknesses:

(1) Throughout the text on figures, labels are nearly impossible to read. I had to zoom into the PDF to determine what the figure was showing. Please make text in all figures a minimum of 10 point font. Similarly, Figure 2D point type is impossible to read. Points should be larger in all figures. Gene names should be in italics in all figures, following C. elegans convention.

(2) I have a strong bias against the second point in Figure 1A. Sequencing of trios, cohorts, or individuals NEVER identifies causal genes in the disease. This technique proposes a candidate gene. Future experiments (oftentimes in model organisms) are required to make those connections to causality. Please edit this figure and parts of the text.

(3) How were the high-confidence orthologs filtered from 767 to 543 (lines 128-131)? Also, the choice of the final list of 25 genes is not well justified. Please expand more about how these

choices were made.

(4) Figures 3 and 4, why show all 8289 features? It might be easier to understand and read if only the 256 Tierpsy features were plotted in the heat maps.

(5) The unc-80 mutant screen is clever. In the feature space, it is likely better to focus on the 256 less-redundant Tierpsy features instead of just a number of features. It is unclear to me how many of these features are correlated and not providing more information. In other words, the "worsening" of less-redundant features is far more of a concern than "worsening" of 1000 correlated features.Reviewer #2 (Public review):

Summary and strengths:

O'Brien et al. present a compelling strategy to both understand rare disease that could have a neuronal focus and discover drugs for repurposing that can affect rare disease phenotypes. Using C. elegans, they optimize the Brown lab worm tracker and Tierpsy analysis platform to look at movement behaviors of 25 knockout strains. These gene knockouts were chosen based on a process to identify human orthologs that could underlie rare diseases. I found the manuscript interesting and a powerful approach to make genotype-phenotype connections using C. elegans. Given the rate that rare Mendelian diseases are found and candidate genes suggested, human geneticists need to consider orthologous approaches to understand the disease and seek treatments on a rapid time scale. This approach is one such way. Overall, I have a few minor suggestions and some specific edits.

Weaknesses:

(1) Throughout the text on figures, labels are nearly impossible to read. I had to zoom into the PDF to determine what the figure was showing. Please make text in all figures a minimum of 10 point font. Similarly, Figure 2D point type is impossible to read. Points should be larger in all figures. Gene names should be in italics in all figures, following C. elegans convention.

(2) I have a strong bias against the second point in Figure 1A. Sequencing of trios, cohorts, or individuals NEVER identifies causal genes in the disease. This technique proposes a candidate gene. Future experiments (oftentimes in model organisms) are required to make those connections to causality. Please edit this figure and parts of the text.

(3) How were the high-confidence orthologs filtered from 767 to 543 (lines 128-131)? Also, the choice of the final list of 25 genes is not well justified. Please expand more about how these choices were made.

(4) Figures 3 and 4, why show all 8289 features? It might be easier to understand and read if only the 256 Tierpsy features were plotted in the heat maps.

(5) The unc-80 mutant screen is clever. In the feature space, it is likely better to focus on the 256 less-redundant Tierpsy features instead of just a number of features. It is unclear to me how many of these features are correlated and not providing more information. In other words, the "worsening" of less-redundant features is far more of a concern than "worsening" of 1000 correlated features.

https://doi.org/10.7554/eLife.92491.2.sa2

Reviewer #3 (Public review):

In this study, O'Brien et al. address the need for scalable and cost-effective approaches to finding lead compounds for the treatment of the growing number of Mendelian diseases. They used state-of-the-art phenotypic screening based on an established high-dimensional phenotypic analysis pipeline in the nematode C. elegans.

First, a panel of 25 C. elegans models was created by generating CRISPR/Cas9 knock-out lines for conserved human disease genes. These mutant strains underwent behavioral analysis using the group's published methodology. Clustering analysis revealed common features for genes likely operating in similar genetic pathways or biological functions. The study also presents results from a more focused examination of ciliopathy disease models.

Subsequently, the study focuses on the NALCN channel gene family, comparing the phenotypes of mutants of nca-1, unc-77, and unc-80. This initial characterization identifies three behavioral parameters that exhibit significant differences from the wild type and could serve as indicators for pharmacological modulation.

As a proof-of-concept, O'Brien et al. present a drug repurposing screen using an FDA-approved compound library, identifying two compounds capable of rescuing the behavioral phenotype in a model with UNC80 deficiency. The relatively short time and low cost associated with creating and phenotyping these strains suggest that high-throughput worm tracking could serve as a scalable approach for drug repurposing, addressing the multitude of Mendelian diseases. Interestingly, by measuring a wide range of behavioural parameters, this strategy also simultaneously reveals deleterious side effects of tested drugs that may confound the analysis.

Considering the wealth of data generated in this study regarding important human disease genes, it is regrettable that the data is not made accessible to researchers less versed in data analysis methods. This diminishes the study's utility. It would have a far greater impact if an accessible and user-friendly online interface were established to facilitate data querying and feature extraction for specific mutants. This would empower researchers to compare their findings with the extensive dataset created here.

Another technical limitation of the study is the use of single alleles. Large deletion alleles were generated by CRISPR/Cas9 gene editing. At first glance, this seems like a good idea because it limits the risk that background mutations, present in chemically-generated alleles, will affect behavioral parameters. However, these large deletions can also remove non-coding RNAs or other regulatory genetic elements, as found, for example, in introns. Therefore, it would be prudent to validate the behavioral effects by testing additional loss-of-function alleles produced through early stop codons or targeted deletion of key functional domains.

https://doi.org/10.7554/eLife.92491.2.sa1

Author response:

The following is the authors' response to the original reviews.

> ***Public Reviews:***
>
> ***Reviewer #1 (Public Review):***
>
> *Summary:*
>
> *As the scientific community identifies increasing numbers of genetic variants that cause rare human diseases, a challenge is how the field can most quickly identify pharmacological interventions to address known deficits. The authors point out that defining phenotypic outcomes required for drug screen assays is often challenging, and emphasize how invertebrate models can be used for quick ID of compounds that may address genetic deficits. A major contribution of this work is to establish a framework for potential intervention drug screening based on quantitative imaging of morphology and*

> *mobility behavior, using methods that the authors show can define subtle phenotypes in a high proportion of disease gene knockout mutants.*
>
> *Overall, the work constitutes an elegant combination of previously developed high-volume imaging with highly detailed quantitative phenotyping (and some paring down to specific phenotypes) to establish proof of principle on how the combined applications can contribute to screens for compounds that may address specific genetic deficits, which can suggest both mechanism and therapy.*
>
> *In brief, the authors selected 25 genes for which loss of function is implicated in human neuro-muscular disease and engineered deletions in the corresponding C. elegans homologs. The authors then imaged morphological features and behaviors prior to, during, and after blue light stimuli, quantitating features, and clustering outcomes as they elegantly developed previously (PMID 35322206; 30171234; 30201839). In doing so, phenotypes in 23/25 tested mutants could be separated enough to distinguish WT from mutant and half of those with adequate robustness to permit high-throughput screens, an outcome that supports the utility of general efforts to ID phenotypes in C. elegans disease orthologs using this approach. A detailed discussion of 4 ciliopathy gene defects, and NACLN-related channelopathy mutants reveals both expected and novel phenotypes, validating the basic approach to modeling vetted targets and underscoring that quantitative imaging approaches reiterate known biology. The authors then screened a library of nearly 750 FDA-approved drugs for the capacity to shift the unc-80 NACLN channel-disrupted phenotype closer to the wild type. Top "mover" compound move outcome in the experimental outcome space; and also reveal how "side effects" can be evaluated to prioritize compounds that confer the fewest changes of other parameters away from the center.*
>
> *Strengths:*
>
> *Although the imaging and data analysis approaches have been reported and the screen is limited in scope and intervention exposure, it is important that the authors strongly combine individual approach elements to demonstrate how quantitative imaging phenotypes can be integrated with C. elegans genetics to accelerate the identification of potential modulators of disease (easily extendable to other goals). Generation of deletion alleles and documentation of their associated phenotypes (available in supplemental data) provide potentially useful reagents/data to the field. The capacity to identify "over-shooting" of compound applications with suggestions for scale back and to sort efficacious interventions to minimize other changes to behavioral and physical profiles is a strong contribution.*
>
> *Weaknesses:*
>
> *The work does not have major weaknesses, although it may be possible to expand the discussion to increase utility in the field:*
>
> *(1) Increased discussion of the challenges and limitations of the approach may enhance successful adaptation application in the field.*
>
> *It is quite possible that morphological and behavioral phenotypes have nothing to do with disease mechanisms and rather reflect secondary outcomes, such that positive hits will address "off-target" consequences.*

This is possible and can only be determined with human data. We now discuss the possibility in the discussion.

> *The deletion approach is adequately justified in the text, but the authors may make the point somewhere that screening target outcomes might be enhanced by the inclusion of*

> *engineered alleles that match the human disease condition. Their work on sod-1 alleles (PMID 35322206) might be noted in this discussion.*

We agree and now mention this work in the discussion. We are currently working on a collection of strains with patient-specific mutations.

> *Drug testing here involved a strikingly brief exposure to a compound, which holds implications for how a given drug might engage in adult animals. The authors might comment more extensively on extended treatments that include earlier life or more extended targeting. The assumption is that administering different exposure periods and durations, but if the authors are aware as to whether there are challenges associated with more prolonged applications, larger scale etc. it would be useful to note them.*

More prolonged applications are definitely possible. We chose short treatments for this screen to model the potential for changing neural phenotypes once developmental effects of the mutation have already occurred. We now briefly discuss this choice and the potential of longer treatments in the discussion.

> *(2) More justification of the shift to only a few target parameters for judging compound effectiveness.*
>
> *- In the screen in Figure 4D and text around 313, 3 selected core features of the unc-80 mutant (fraction that blue-light pause, speed, and curvature) were used to avoid the high replicate requirements to identify subtle phenotypes. Although this strategy was successful as reported in Figure 5, the pared-down approach seems a bit at odds with the emphasis on the range of features that can be compared mutant/wt with the author's powerful image analysis. Adding details about the reduced statistical power upon multiple comparisons, with a concrete example calculated, might help interested scientists better assess how to apply this tool in experimental design.*

To empirically test the effect of including more features on the subsequent screen, we have repeated the analysis using increasing numbers of features. In a new supplementary figure we find increasing the number of features reduces our power to detect rescue. At 256 features, we would not be able to detect any compounds that rescued the disease model phenotype.

> *(3) More development of the side-effect concept. The side effects analysis is interesting and potentially powerful. Prioritization of an intervention because of minimal perturbation of other phenotypes might be better documented and discussed a bit further; how reliably does the metric of low side effects correlate with drug effectiveness?*

Ultimately this can only be determined with clinical trial data on multiple drugs, but there are currently no therapeutic options for UNC80 deficiency in humans. We have included some extra discussion of the side effect concept.

> ***Reviewer #2 (Public Review):***
>
> *Summary and strengths:*
>
> *O'Brien et al. present a compelling strategy to both understand rare disease that could have a neuronal focus and discover drugs for repurposing that can affect rare disease phenotypes. Using C. elegans, they optimize the Brown lab worm tracker and Tierpsy analysis platform to look at the movement behaviors of 25 knockout strains. These gene knockouts were chosen based on a process to identify human orthologs that could underlie rare diseases. I found the manuscript interesting and a powerful approach to*

> *making genotype-phenotype connections using C. elegans. Given the rate at which rare Mendelian diseases are found and candidate genes suggested, human geneticists need to consider orthologous approaches to understand the disease and seek treatments on a rapid time scale. This approach is one such way. Overall, I have a few minor suggestions and some specific edits.*
>
> *Weaknesses:*
>
> *(1) Throughout the text on figures, labels are nearly impossible to read. I had to zoom into the PDF to determine what the figure was showing. Please make text in all figures a minimum of 10-point font. Similarly, the Figure 2D point type is impossible to read. Points should be larger in all figures. Gene names should be in italics in all figures, following C. elegans convention.*

We have updated all figures with larger labels and, where necessary, split figures to allow for better readability. We've also corrected italicisation.

> *(2) I have a strong bias against the second point in Figure 1A. Sequencing of trios, cohorts, or individuals NEVER identifies causal genes in the disease. This technique proposes a candidate gene. Future experiments (oftentimes in model organisms) are required to make those connections to causality. Please edit this figure and parts of the text.*

We have removed references to causation. We were thinking of cases where a known variant is found in a patient where causality has already been established rather than cases of new variant discovery.

> *(3) How were the high-confidence orthologs filtered from 767 to 543 (lines 128-131)? Also, the choice of the final list of 25 genes is not well justified. Please expand more about how these choices were made.*

We now explain the extra keyword filtering step. For the final filtering step, we simply examined the list and chose 25. There is therefore little justification to provide and we acknowledge these cannot be seen as representative of the larger set according to well-defined rules. The choice was based on which genes we thought would be interesting using their descriptions or our prior knowledge ("subjective interestingness" in the main text).

> *(4) Figures 3 and 4, why show all 8289 features? It might be easier to understand and read if only the 256 Tierpsy features were plotted in the heat maps.*

In this case, we included all features because they were all tested for differences between mutants and controls. By consistently using all features for each fingerprint we can be sure that the features that are different that we want to highlight in box plots can be referred to in the fingerprint.

> *(5) The unc-80 mutant screen is clever. In the feature space, it is likely better to focus on the 256 less-redundant Tierpsy features instead of just a number of features. It is unclear to me how many of these features are correlated and not providing more information. In other words, the "worsening" of less-redundant features is far more of a concern than the "worsening" of 1000 correlated features.*

This is a good point. We've redone the analysis using the Tierpsy 256 feature set and included this as a supplementary figure. We find that the same trend exists when looking at this reduced feature set.

> ***Reviewer #3 (Public Review):***
>
> *In this study, O'Brien et al. address the need for scalable and cost-effective approaches to finding lead compounds for the treatment of the growing number of Mendelian diseases. They used state-of-the-art phenotypic screening based on an established high-dimensional phenotypic analysis pipeline in the nematode C. elegans.*
>
> *First, a panel of 25 C. elegans models was created by generating CRISPR/Cas9 knock-out lines for conserved human disease genes. These mutant strains underwent behavioral analysis using the group's published methodology. Clustering analysis revealed common features for genes likely operating in similar genetic pathways or biological functions. The study also presents results from a more focused examination of ciliopathy disease models.*
>
> *Subsequently, the study focuses on the NALCN channel gene family, comparing the phenotypes of mutants of nca-1, unc-77, and unc-80. This initial characterization identifies three behavioral parameters that exhibit significant differences from the wild type and could serve as indicators for pharmacological modulation.*
>
> *As a proof-of-concept, O'Brien et al. present a drug repurposing screen using an FDA-approved compound library, identifying two compounds capable of rescuing the behavioral phenotype in a model with UNC80 deficiency. The relatively short time and low cost associated with creating and phenotyping these strains suggest that high-throughput worm tracking could serve as a scalable approach for drug repurposing, addressing the multitude of Mendelian diseases. Interestingly, by measuring a wide range of behavioural parameters, this strategy also simultaneously reveals deleterious side effects of tested drugs that may confound the analysis.*
>
> *Considering the wealth of data generated in this study regarding important human disease genes, it is regrettable that the data is not actually made accessible. This diminishes the study's utility. It would have a far greater impact if an accessible and user-friendly online interface were established to facilitate data querying and feature extraction for specific mutants. This would empower researchers to compare their findings with the extensive dataset created here. Otherwise, one is left with a very limited set of exploitable data.*

We have now made the feature data available on Zenodo (https://doi.org/10.5281/zenodo.12684118) as a matrix of feature summaries and individual skeleton timeseries data (the feature matrix makes it more straightforward to extract the data from particular mutants for reanalysis). We have also created a static html version of the heatmap in Figure 2 containing the entire behavioural feature set extracted by Tierpsy. This can be opened in a browser and zoomed for detailed inspection. Mousing over the heatmap shows the names of features at each position making it easier to arrive at intuitive conclusions like ‘strain A is slow’ or ‘strain B is more curved’.

> *Another technical limitation of the study is the use of single alleles. Large deletion alleles were generated by CRISPR/Cas9 gene editing. At first glance, this seems like a good idea because it limits the risk that background mutations, present in chemically-generated alleles, will affect behavioral parameters. However, these large deletions can also remove non-coding RNAs or other regulatory genetic elements, as found, for example, in introns. Therefore, it would be prudent to validate the behavioral effects by testing additional loss-of-function alleles produced through early stop codons or targeted deletion of key functional domains.*

We have added a note in the main text on limitations of deletion alleles. We like the idea of making multiple alleles in future studies, especially in cases where a project is focussed on

just one or a few genes.

> ***Recommendations for the authors***
>
> ***Reviewer #1 (Recommendations For The Authors):***
>
> *Note that none of the above suggestions or the one immediately below are considered mandatory.*
>
> *One additional minor point: The dual implication of mevalonate perturbations for NACLM deficiencies is striking. At the same time, the mevalonate pathway is critical for embryo viability among other things, which prompts questions about how reproductive physiology is integrated in this screen approach. It appears that sterilization protocols are not used to prepare screen target animals, but it would be useful to know if there were a signature associated with drug-induced sterility that might help identify one potential common non-interesting outcome of compound treatments in general. In this work, the screen treatment is only 4 hours, which is probably too short to compromise reproduction, but as noted above, it is likely users would intend to expose test subjects for much longer than 4-hour periods.*

This is an interesting point. In its current form our screen doesn't assess reproductive physiology. This is something that we will consider in ongoing projects.

> *Figures*
>
> *Figure 1D might be omitted or moved to supplement.*

We have removed 1D and moved figure 1E as a standalone table (Table 1) to improve readability.

> *Figure 2D "key" is hard to make out size differences for prestim, bluelight, and poststim - more distinctive symbols should be used.*

We have increased the size of the symbols so that the key is easier to read.

> *Line 412 unc-25 should be in italics*

Corrected

> ***Reviewer #2 (Recommendations For The Authors):***
>
> *Specific edits:*

All of the errors below have been corrected.

> *Line 47, "loss of function" should be hyphenated because it is a compound adjective that modifies mutations.*
>
> *Line 50, "genetically-tractable" should not be hyphenated because it is not a compound adjective. It is an adverb-adjective pair. Line 102 has the same grammatical issue.*
>
> *Line 85, "rare genetic diseases" do not "affect nervous system function". The disease might have deficits in this function, but the disease does not do anything to function.*
>
> *Line 86, it should be mutations not mutants. Mutations are changes to DNA. Mutants are individuals with mutations.*

> *Throughout, wild-type should be hyphenated when it is used as a compound adjective.*
>
> *Figure 4, asterisks is spelled incorrectly.*
>
> ***Reviewer #3 (Recommendations For The Authors):***
>
> *- As stated in the public review, the utility of the study is limited by the lack of access to the complete dataset. The wealth of data produced by the study is one of its major outputs.*

We have made the data publicly available on Zenodo. We appreciate the request.

> *- Describe the exact break-points of the different alleles, because it was not readily feasible to derive them from the gene fact sheets provided in the supplementary materials.*

We have now provided the start position and total length of deletion for each gene in the gene fact sheets.

> *- Figure 1C: what does "Genetic homology"/"sequence identity" refer to? How were these values calculated?*
>
> *UNC-49 is clearly not 95% identical to vertebrate GABAR subunits at the protein level.*

We have changed the axis label to “BLAST % Sequence Identity” to clarify that these values are calculated from BLAST sequence alignments on WormBase and the Alliance Genom Resources webpages.

> *- Figure 1E : The data presented in Figure 1E appears somewhat unreliable. For example, a cursory check showed:*
>
> *(1) Wrong human ortholog: unc-49 is a Gaba receptor, not a Glycine receptor as indicated in the second column.*
>
> *(2) Wrong disease association: dys-1 is not associated with Bardet-Biedl syndrome; overall the data indicated in the table does not seem to fully match the HPO database.*
>
> *(3) Inconsistent disease association: why don't the avr-14 and glc-2 (and even unc-49) profiles overlap/coincide given that they present overlapping sets of human orthologs.*

Thank you for catching this! We have corrected gene names which were mistakenly pasted. We have also made this a standalone table (Table 1) for improved readability.

> *- Error in legend to figure 4I : "with ciliopathies and N2" > ciliopathies should be "NALCN disease".*
>
> *- Error at line 301: "Figures 2E-H" should be "Figures 4E-H".*

Corrected.

https://doi.org/10.7554/eLife.92491.2.sa0